

# Fragility assessment for roof sheathing failure in high wind regions

Kyung Ho Lee, David V. Rosowsky\*

*Department of Civil Engineering, Texas A&M University, College Station, TX 77843-3136, USA*

Received 19 July 2004; received in revised form 2 December 2004; accepted 20 December 2004

Available online 4 March 2005

## Abstract

This paper presents a fragility assessment for roof sheathing in light frame constructions built in high wind regions. A fragility methodology is developed to assess the performance of roof sheathing subjected to uplift (suction) pressures. The majority of single-family housing in the United States is woodframe construction. A review of the performance of woodframe buildings after recent hurricanes has shown that the majority of wind damage (insured losses) was the result of a breach in the building envelope. Loss of roof sheathing and broken windows result in water penetration causing extensive interior damage and associated property and contents losses. The aim of this study was to develop a fragility model for roof sheathing uplift using available fastener test data, recently developed wind load statistics, and a code-based approach for evaluating pressures. Five baseline structures considering different roof shapes, geographic locations, nail types, and enclosure conditions were investigated using simulation and system reliability concepts. Fragilities and complementary fragilities (or survivorship curves) of roof sheathing removal considering different levels of damage are developed as a function of basic wind speed (3 s gust wind speed at 33 ft (10 m) above the ground in open terrain). The fragility models presented in this paper can be used to develop performance-based design guidelines for woodframe structures as well as tools for condition assessment and loss estimation for use with the existing building inventory.

© 2005 Elsevier Ltd. All rights reserved.

**Keywords:** Fragility; Performance-based design; Probability; Roof sheathing; Wind; Wood

## 1. Introduction

The majority of single-family housing in the United States is woodframe construction. Woodframe buildings are among the most vulnerable structures to high wind hazards. A review of the performance of woodframe buildings following recent hurricanes has shown that the majority of wind damage and consequent insurance losses are the result of a breach in the building envelope. Water penetration through the building envelope and broken windows, resulting in extensive interior damage as well as damage to contents, causes the majority of economic losses. Hurricane Hugo (1989) cost insurance companies US\$5.4 billion, most of which was residential damage claims. Hurricane Andrew (1992) produced insured property losses estimated at US\$17.7 billion; Hurricane Iniki (1992) caused

US\$1.8 billion in damage. Damage due to Hurricane Opal (1995) was close to US\$2.2 billion.<sup>1</sup> Increased population growth in hurricane-prone regions, i.e. along the Southeast and Gulf coasts of the US and Hawaii, likely will result in even greater losses in the future.

The main objective of design codes and standards is to protect public (life) safety by preventing structural collapse or failure during rare events in a building's lifetime. While this objective has largely been achieved for buildings in the US subjected to hurricane windstorms, economic losses and social disruption related to hurricane events are still unacceptable. This has led to current trends toward a new design philosophy (called performance-based design) in which the structural system is designed to meet specific performance criteria under different hazard levels [5].

\* Corresponding author.

E-mail address: [rosowsky@tamu.edu](mailto:rosowsky@tamu.edu) (D.V. Rosowsky).

<sup>1</sup> These estimates were obtained from the *Georgia Insurance Information Service* ([www.giis.org](http://www.giis.org)).

The basic concept of performance-based design is to design a structure so that it will perform in a specified manner when subjected to various loading scenarios. Therefore, designers can design structures capable of providing reasonable levels of protection against various hazard levels. Performance-based design will require more comprehensive and quantitative probability-based procedures for managing risk and uncertainty than are found in first-generation criteria such as LRFD [5]. Fragility analysis procedures for roof sheathing attachment can be used for both design and assessment of woodframe structures built in high wind regions. This paper presents a fragility methodology for assessing the response of roof sheathing subject to specified demands from extreme wind loading.

## 2. LRFD and PBD

Beginning with the general load requirements in American National Standards Institute (ANSI) Standard A58 [3], probabilistic-based limit state design (now called Load and Resistance Factor Design, or LRFD, in the US) has been developed and is widely used. Recently, the joint American Forest & Paper Association/American Society of Civil Engineers (AF&PA/ASCE) Standard 16-95 for engineered wood construction adopted the LRFD design format. In LRFD engineered wood structures, the structural safety performance requirement is expressed by a set of equations (ASCE Standard 16-95),

$$\lambda\phi R' > \sum \gamma_i Q_i \quad (1)$$

where  $R'$  = adjusted resistance of a member, component or connection,  $\phi$  = resistance factor that takes into account variability in short-term strength, and  $\lambda$  = a time-effect factor that takes into account loss of strength under long-term duration of load. On the right-hand side of Eq. (1),  $Q_i$  = load effect (moment, shear or axial) due to nominal load  $i$ , and  $\gamma_i$  = load factor that takes into account variability in load  $i$ . Nominal loads and load factors are defined in ASCE 7-02 (2002). The structural safety performance requirement expressed by Eq. (1) is a limit criterion beyond which the structural member is judged to be unsafe or nonfunctional.

Although the LRFD design process has many advantages relative to allowable strength design (ASD), it has several shortcomings, particularly for woodframe buildings [5,12].

1. The design and calibration process using LRFD was performed only for individual members, components or connections. It is therefore hard to predict the structural system behavior under severe natural hazards such as extreme wind events or earthquakes.
2. LRFD design focuses on the life safety objective. There has been little attention paid to serviceability issues, which do not impact structural safety but may have a significant social and economic impact.

3. LRFD design cannot ensure that hazards are treated consistently.

Recent natural disasters in the US and elsewhere around the world have highlighted the social, political, and economic ramifications of the traditional view of codes (to prevent structural collapse during rare events), as economic disruptions caused by structural or member failures have not been deemed acceptable by the public. Performance-based engineering is a new paradigm in which the design process for the purpose of meeting performance expectations (limit states) of the building occupants, owner, and the public. To achieve reasonable agreement between calculated and observed failure rates, properly validated system reliability analysis models are essential [12]. Seismic performance-based engineering concepts for woodframe buildings are starting to be developed [5,13]. As indicated previously, woodframe buildings are among the most vulnerable types of structures to high wind hazards. The enormous economic losses in recent hurricanes were generally the results of building envelope failure, most typically roof sheathing loss or broken windows. This paper presents a fragility methodology for assessing the response of roof sheathing subjected to specified demands from extreme wind loading.

## 3. Fragility modeling

A fragility can be defined as the conditional probability of failure of a structural member or system for a given set of input variables [7]. It is expressed as:

$$P[LS] = \sum_{\text{all } D} P[LS|D = x]P[D = x] \quad (2)$$

where  $D$  = a random demand on the system (e.g., 3 s gust wind speed, spectral acceleration, flood level);  $P[LS|D = x]$  is the conditional probability of the limit state ( $LS$ ) at given demand  $x$ . The hazard is defined by the probability,  $P[D = x]$ . The conditional probability,  $P[LS|D = x]$  is the fragility. Eq. (2) also can be expressed in convolution integral form if the hazard is a continuous function of demand  $x$ :

$$P[LS] = \int_0^\infty Fr(x)g_X(x) dx \quad (3)$$

where  $Fr(x)$  = fragility function of demand  $x$  expressed in the form of a cumulative distribution function and  $g_X(x)$  = hazard function expressed in the form of a probability density function.

The fragility of a structural system commonly is modeled using a lognormal distribution,

$$Fr(x) = \Phi \left[ \frac{\ln(x) - \lambda_R}{\xi_R} \right] \quad (4)$$

in which  $\Phi[\bullet]$  = standard normal cumulative distribution function,  $\lambda_R$  = logarithmic median of capacity  $R$  (in units that are dimensionally consistent with demand), and  $\xi_R$  = logarithmic standard deviation of capacity  $R$ . Hazard curves

Table 1  
Dimensions and characteristics of baseline houses

Properties	Type 1	Type 2	Type 3	Type 4	Type 5
Plan dimension	22.6 ft × 40 ft (6.9 m × 12.2 m)	28.0 ft × 40 ft (8.5 m × 12.2 m)	28.0 ft × 40 ft (8.5 m × 12.2 m)	28.0 ft × 40 ft (8.5 m × 12.2 m)	30 ft × 38 ft (9.1 m × 11.6 m)
No. of stories	1	1	2	1	1
Roof type	Gable	Gable	Gable	Hip	Hip
Roof slope	4:12 (18.4°)	6:12 (26.6°)	8:12 (33.7°)	4:12 (18.4°)	6:12 (26.6°)
Roof framing spacing	24 in. (61 cm)	24 in. (61 cm)	24 in. (61 cm)	24 in. (61 cm)	24 in. (61 cm)
Overhang	None	12 in. (30.5 cm)	12 in. (30.5 cm)	None	12 in. (30.5 cm)

can be determined using statistical analysis or, in the case of seismic hazard, may be obtained from agencies such as the US Geologic Survey. A system fragility can be obtained through a probabilistic analysis of the system. Fragilities can be used to identify a level of demand that a component or system will withstand with certain probability. Fragility curves can be used in both design and condition assessment applications [5].

#### 4. Fragility model for roof sheathing subjected to wind load

##### 4.1. Description of baseline structures

Fragility assessments were performed for light-frame wood structures with various roof geometries (e.g., roof type, roof slope, roof height, roof truss or framing spacing, overhang), construction practices (e.g., nail type, nailing pattern), and other factors (e.g., exposure condition) subjected to wind loads. In this study, five baseline houses were considered, designated Type 1–5. These five types of single-family light-frame residential buildings were considered to be representative of much of the residential building inventory in the southeast United States. Type 1 is based on a model that has been used extensively in studies at Clemson University's Wind Load Test Facility [10]. Types 2 and 3 have been considered in a recent study by the National Association of Home Builders [9]. Type 1, 2, and 3 are all gable roof type buildings. Gable roofs are the most popular roof type for woodframe residential buildings in the United States. Type 4 and 5 are hip roof type buildings. Hip roofs are the second most widely used system. The five baseline structures are intended to be representative of typical single-family houses built in the US. Dimensions and detailed characteristics are shown in Table 1. The dimensions and roof sheathing panel layouts for the Type 1 baseline structure are shown in Fig. 1. Those for other baseline structures are shown elsewhere [8].

##### 4.2. Limit states

Roof sheathing failure due to wind load occurs when internal and external pressures acting on a panel combine

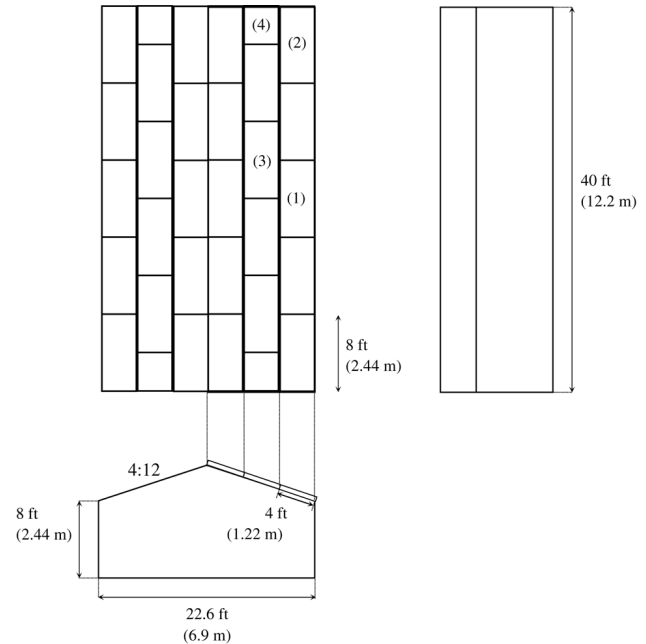


Fig. 1. Dimensions and panel layout showing four panel locations, Structure Type 1.

to cause sufficient uplift on the panel to remove it (multiple nail withdrawal) from the roof framing. Considerable information on this failure mode is available in the literature (e.g., [11,14]). Roof sheathing uplift failure is influenced by three major parameters: resistance, wind load, and dead load. Resistance capacity generally is provided by nails, wind load refers to the uplift pressure acting on the panel, and dead load is the self-weight of roof sheathing panel (and coverings) acting in a direction opposite to the uplift pressures. The limit state function for one piece of roof sheathing uplift can be written in terms of the basic (random) variables as:

$$g(x) = R - (W - D) \quad (5)$$

where  $R$  = uplift resistance capacity of the nailed roof sheathing panel,  $W$  = wind load acting on the sheathing panel, and  $D$  = dead load. Sheathing panel failure can be defined as the condition where  $g(x) < 0$ . The wind load, and hence the failure probability, is a function of the basic wind speed ( $V$ ) squared (see Eqs. (7a) and (7b)). It should

Table 2  
Summary of resistance statistics

Nail type/spacing	Panel size	Mean	COV	CDF	References
8d nail <sup>a</sup> 6 in./12 in. (15.2 cm/30.5 cm)	4 ft × 8 ft (1.22 m × 2.44 m)	57.7 psf (2.76 kN/m <sup>2</sup> )	0.20	Normal	[11,14]
	4 ft × 4 ft (1.22 m × 1.22 m)	73.3 psf (3.51 kN/m <sup>2</sup> )	0.20	Normal	
6d nail <sup>b</sup> 6 in./12 in. (15.2 cm/30.5 cm)	4 ft × 8 ft (1.22 m × 2.44 m)	25.0 psf (1.20 kN/m <sup>2</sup> )	0.15	Normal	
	4 ft × 4 ft (1.22 m × 1.22 m)	32.0 psf (1.53 kN/m <sup>2</sup> )	0.15	Normal	

<sup>a</sup> 0.131 in. (3.33 mm) diameter, 2.5 in. (63.5 mm) long.

<sup>b</sup> 0.113 in. (2.87 mm) diameter, 2.0 in. (50.8 mm) long.

be noted that dead load ( $D$ ) in Eq. (5) counteracts the uplift of the wind, and has a beneficial effect on roof sheathing performance. Often in light-frame structures, this dead load is relatively small and may be conservatively ignored, thereby simplifying the limit state function. In this paper, dead load is included in Eq. (5). System limit states were defined in this study to correspond to four different levels of damage: no damage (number of sheathing panel failures = 0), no more than one sheathing damage (number of sheathing panel failures  $\leq 1$ ), fewer than 10% of sheathing panels failed, and fewer than 25% of sheathing panels failed. Three different wind directionality cases were considered in this study: (1) all possible directions, using a directionality factor, (2) normal-to-ridge, and (3) parallel-to-ridge. The latter two cases do not require a directionality factor. These three directionality cases cover all possible wind direction scenarios for the bi-symmetric simple rectangular baseline structures considered in this study.

#### 4.3. Uplift capacity (resistance) statistics

The statistics assumed for uplift capacity of typical full-size roof sheathing panels of representative materials and attached using common practices are shown in Table 2. These statistics were obtained from previous studies including both experimental and analytical components [11,14]. For this study, statistics were obtained for uplift capacity of individual roof sheathing panels, both 4 ft × 8 ft (1.22 m × 2.44 m) and 4 ft × 4 ft (1.22 m × 1.22 m) in size, consisting of 15/32 in. (12 mm) CDX plywood attached with smooth-shank hand-driven 8d common nails (0.131 in. (3.33 mm) diameter, 2.5 in. (63.5 mm) long) or 6d common nails (0.113 in. (2.87 mm) diameter, 2.0 in. (50.8 mm) long), to nominal 2 in. × 4 in. (50 mm × 100 mm) spruce-pine-fir (SPF) rafters spaced 24 in. (610 mm) on-center. The nailing schedule was 6 in. (150 mm) along the edge of the panel and 12 in. (300 mm) at interior locations [11].

#### 4.4. Dead load statistics

Dead load considered in this study is the self-weight of the roof sheathing panel. It is assumed to remain constant. The mean and COV of the dead load, which

acts in a direction opposite to the wind uplift, is taken as 3.5 psf (168 N/m<sup>2</sup>) and 0.10, respectively. These values were based on estimated weights of materials and assumed values of mean-to-nominal and COV of 1.05 and 0.10, respectively [3]. The dead load is assumed to be normally distributed.

#### 4.5. Wind load statistics

ASCE 7-02 [1] defines two types of structural elements subjected to wind load: (1) main wind-force resisting systems (MWFRS), and (2) components and cladding (C&C). Different elements have different effective tributary areas as well as different wind pressure coefficients. A main wind-force resisting system is considered an assemblage of structural elements that work together to provide support and stability for the overall structure. Components and cladding elements are defined as elements of the building envelope that transfer the load to the main wind-force resisting system. Individual sheathing panels can be assumed to perform as individual components being loaded directly by the wind, with equivalent tributary area for a critical location of a roof panel on the order of 1–2 ft<sup>2</sup> (0.093–0.186 m<sup>2</sup>), the tributary area of an individual fastener [14]. Wind pressures acting on the roof sheathing panels therefore were calculated using the C&C provisions in ASCE 7-02. The wind pressure acting on components and cladding for low-rise structures in ASCE 7-02 (Eqs. 6–22) is determined from:

$$W = q_h [GC_p - GC_{pi}] \quad (6)$$

where  $q_h$  = velocity pressure evaluated at mean roof height ( $h$ ),  $GC_p$  = product of gust factor and external pressure coefficient, and  $GC_{pi}$  = product of gust factor and internal pressure coefficient. The velocity pressure evaluated at height ( $z$ ) in ASCE 7-02 (Eqs. (6)–(15)) is given by:

$$q_z = 0.00256 K_z K_{zt} K_d V^2 I \quad (\text{units: lb/ft}^2; V \text{ in mph}) \quad (7a)$$

$$q_z = 0.613 K_z K_{zt} K_d V^2 I \quad (\text{units: N/m}^2; V \text{ in m/s}) \quad (7b)$$

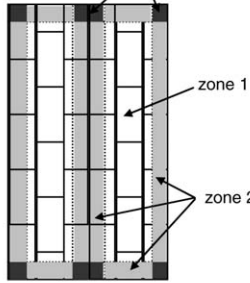
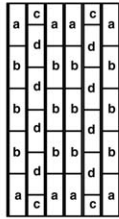
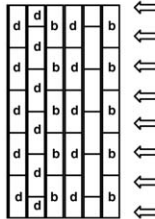
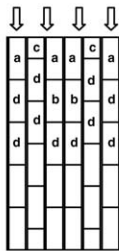
where  $q_z$  is equivalent to  $q_h$  at the mean roof height,  $K_z$  = the velocity pressure exposure factor,  $K_{zt}$  = the topographic factor,  $K_d$  = the wind directionality factor,  $V$  = the basic wind speed in mph (3 s gust wind speed at 33 ft (10 m) and in open terrain) (Eq. (7a)) and in m/s (Eq. (7b)), respectively, and  $I$  = the importance factor. Wind effects on low-rise

Table 3  
Summary of wind load statistics

Parameters	Category		Nominal	Mean	COV	CDF
$K_z$	Exposure B	0–30 ft (0–9.1 m)	0.70	0.71 <sup>a</sup>	0.19 <sup>a</sup>	Normal
	Exposure C	0–15 ft (0–4.6 m)	0.85	0.82 <sup>a</sup>	0.14 <sup>a</sup>	Normal
		16–20 ft (4.9–6.1 m)	0.90	0.84	0.14	
	Exposure D	0–15 ft (0–4.6 m)	1.03	0.99 <sup>a</sup>	0.14 <sup>a</sup>	Normal
		16–20 ft (4.9–6.1 m)	1.08	1.04 <sup>a</sup>	0.14 <sup>a</sup>	
$K_d$	Components and cladding		0.85	0.89	0.16	Normal
$GC_{pi}$	Enclosed		0.18	0.15 <sup>a</sup>	0.33 <sup>a</sup>	Normal
	Partially enclosed		0.55	0.46 <sup>a</sup>	0.33 <sup>a</sup>	
$GC_p$	see Table 4					Normal
$K_{zt}$	Deterministic (1.0)					
$I$	Deterministic (1.0)					

<sup>a</sup> Modified from Ellingwood and Tekie (1999).

Table 4  
Summary of  $GC_p$  for structure Type 1

nominal $GC_p$ (ASCE 7-02)				Type 1 (roof slope = 18.4°)		
Zone 3	Zone 2	Zone 1		GC <sub>p</sub> values at each panel		
–2.6	–1.7	–0.9		all directions	normal-to-ridge	parallel-to-ridge
						
Nominal <sup>a</sup>	Mean <sup>b</sup>	COV	Number of panels	All directions	Normal-to-ridge direction	Parallel-to-ridge direction
a	–1.861	–1.768	8		0	4
b	–1.532	–1.455	12		10	2
c	–1.500	–1.425	4		0	2
d	–0.900	–0.855	8		16	10
			32		26	18

<sup>a</sup> Calculated using weighted-average method.

<sup>b</sup> Calculated using mean-to-nominal value provided by [4].

buildings are characterized, for the purpose of design, as distributed static loads. The gust pressure coefficient,  $GC_p$ , varies by panel location. For example, panels along the edge of the roof have higher external pressures than the interior panels. Nominal values of  $GC_p$  are determined for each panel using ASCE 7-02. The corresponding random variables are determined using information from ASCE 7-02 and a recent Delphi study [4]. Table 3 summarizes the wind load statistics used in this study.

#### 4.6. Calculation of probability of failure for individual sheathing panel

Before evaluating the reliability of a roof system comprising a collection of sheathing panels, it is necessary to calculate the probability of failure for an individual sheathing panel. The limit state function for an individual sheathing panel is given by Eq. (5). High wind pressures on a low-rise roof occur in the regions of flow separation at



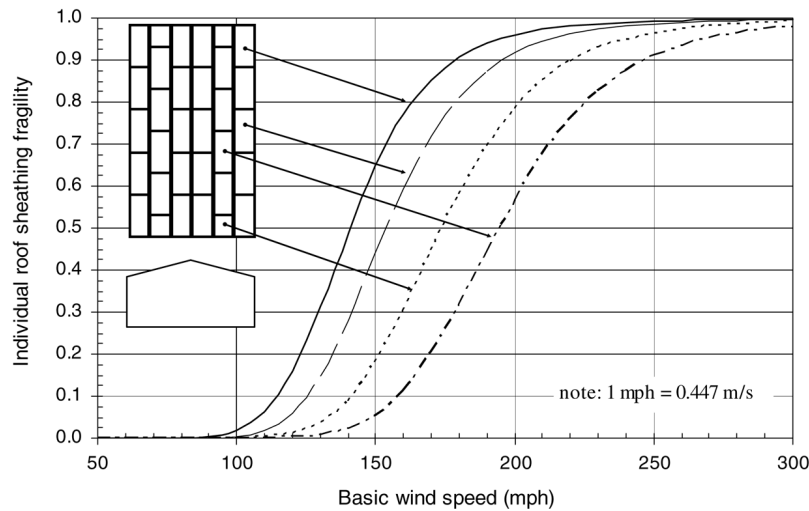


Fig. 2. Fragilities for individual roof sheathing failure (Structure Type 1/Exposure B/8d nail — 6 in./12 in. spacing).

the eave, ridge, and corners at the roof. Change in external wind pressure coefficient,  $GC_p$ , results in different wind pressures at different locations on the roof. ASCE 7 defines three different wind zones (designated zone 1, 2 and 3) with different pressure coefficients. Effective (aggregated) nominal external pressure coefficients for individual panels can be calculated using a weighted-average method (a sum of the external wind pressures on specific zones – e.g., zone 1, 2 or 3 – multiplied by the percentage of sheathing panel area over which those pressures are assumed to act) and statistics (mean-to-nominal and COV) can be established using information provided by Ellingwood and Tekie [4]. The statistics for the product of gust factor and external pressure coefficient,  $GC_p$ , for structure Type 1 is shown in Table 4. An enclosed structure is assumed until first panel failure, after which the structure is assumed to be partially enclosed. (The failure of windows or doors before first panel failure is a possibility, however this is not explicitly considered here. This could be addressed using event-tree analysis if desired.) This assumption is used in the roof sheathing system reliability calculation subsequently.

ASCE 7-02 [1] provides a wind directionality factor (0.85 for components and cladding for ordinary buildings) to account for two effects: (1) the reduced probability of maximum winds coming from any given direction, and (2) the reduced probability of the maximum pressure coefficient occurring for any given wind direction [1]. It may be of interest to compare roof sheathing fragilities calculated with the directionality factor to those evaluated for a particular direction (without the directionality factor). Such a comparison can shed some light on the suitability of current directionality factors and statistics, such as those suggested by Ellingwood and Tekie [4] for components and cladding, e.g., mean = 0.89, COV = 0.16. To make this comparison, roof sheathing fragilities were developed for simple rectangular structures having both gable and

hip roof types considering: (i) all possible directions with directionality factor, (ii) the normal-to-ridge direction without directionality factor, and (iii) the parallel-to-ridge direction without directionality factor. ASCE 7-02 provides the product of gust factor and external pressure coefficient,  $GC_p$ , considering all directions (i.e., an “envelope” of worst-case values). The “map” of pressure coefficients over the roof cannot occur simultaneously at any instant in time. (And only if the eye of a storm with rotational symmetry passes directly over the structure can the roof experience all of those pressures in a single wind event.) It is therefore necessary to understand the external pressure distributions (contours) for the normal-to-ridge and parallel-to-ridge directions, as these would be the worst-case directions. External pressures depend on roof geometry (e.g., roof type, roof angle, plan dimensions, and overhang). Therefore, it is necessary to simplify the external pressure distribution for a particular wind direction. This was done using the work by Cook [2], Holmes [6] and Xu and Reardon [15]. The statistics for  $GC_p$  for each panel were developed using the result from the Delphi study [4] and the nominal (weighted-average) values determined using ASCE 7-02 [1]. Table 4 summarizes the statistics of  $GC_p$  for the Type 1 baseline structure. The statistics of  $GC_p$  for the other baseline structures are provided elsewhere [8].

Individual panel failure fragilities defined by Eq. (2) were evaluated using FORM (First-Order Reliability Method) techniques to evaluate the limit state function given by Eq. (5) using the statistics for wind, dead, and uplift capacity described in previous sections. In the case of structure Type 1, four individual panel types (shown on Fig. 1) were considered: (1) full size 4 ft × 8 ft (1.22 m × 2.44 m) panel located along the long edge of the roof, (2) full size panel located in the corner, (3) full size panel located in the interior, and (4) half-size 4 ft × 4 ft (1.22 m × 1.22 m) panel located along the short edge. Fig. 2 presents the fragility curves for these four individual

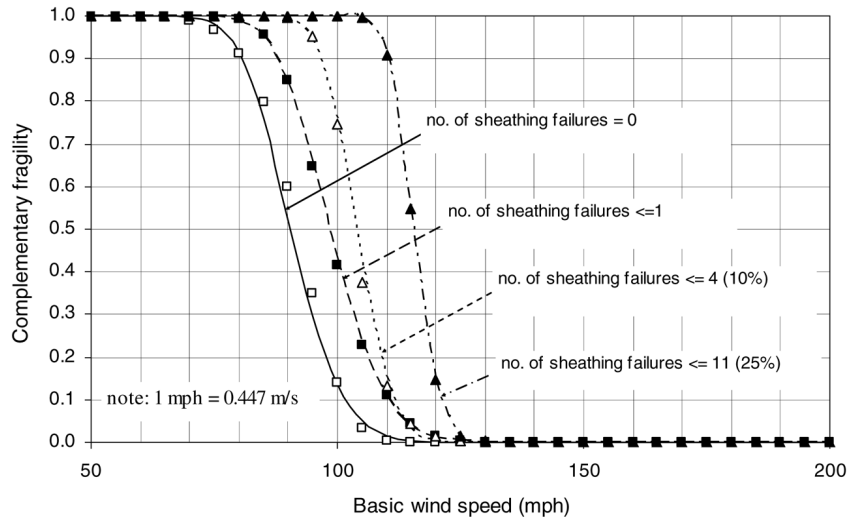


Fig. 3. Lognormal fitted roof system complementary fragilities (Structure Type 2/Exposure C/8d nail — 6 in./12 in. spacing).

sheathing panels in structure Type 1. For the results shown in this figure, roof sheathing is presumed to be attached using 8d common nails (0.131 in. (3.33 mm) diameter, 2.5 in. (63.5 mm) long) spaced at 6 in. (150 mm) along the edge and 12 in. (300 mm) in the interior of the panel, the structure is assumed to be located in Exposure B (suburban residential area with mostly single-family dwellings), and the all possible wind directions case is considered. Panels in these four locations have different external pressures (see Table 4). The individual panel fragility curves are used in the next section to calculate the fragility for complete roof systems.

#### 4.7. Calculation of roof system failure probabilities

In the previous section, the probability of failure of an individual roof sheathing panel (worst-case loading) was investigated. In this section, simple system reliability concepts are utilized to construct fragility curves for limit states defined by failure of multiple roof sheathing panels. Assuming statistically independent panel failures,<sup>2</sup> the CDF for system safety conditioned on wind speed can be written as:

$$F_{\text{system}}(\text{safety}|V) = F_{\text{system}}(N_f = 0|V) = \prod_{i=1}^n (1 - P_i[\text{fail}|V]) \quad (8)$$

where  $V$  = wind speed,  $N_f$  = number of failed panels,  $n$  = total number of panels,  $P_i[\text{fail}|V]$  = failure probability of panel  $i$  given wind speed  $V$ . Eq. (8) can be used to calculate

the fragility (conditional limit state probability) for the case of fewer than one roof sheathing panel failures as:

$$F_{\text{system}}(N_f \leq 1|V) = F_{\text{system}}(N_f = 0|V) + F_{\text{system}}(N_f = 1|V). \quad (9)$$

Similarly, the fragility for the case of fewer than  $j$  roof sheathing panel failures can be written as:

$$F_{\text{system}}(N_f \leq j|V) = \sum_{i=0}^j F_{\text{system}}(N_f = i|V). \quad (10)$$

Since the baseline houses each have at least 30 roof sheathing panels which must be included when considering the case of all wind directions, and at least 10 roof sheathing panels when considering any one wind direction, Eq. (10) can become cumbersome. Numerical simulation can be used to simplify the analysis. The failure of an individual panel was calculated using the simple closed-form procedure described in the previous section. Once the first panel fails, the internal pressure conditions change from those of an “enclosed” structure to those of a “partially enclosed” structure, and the failure probabilities are re-computed using the new pressure coefficients. The system failure probability for each given system limit state at a given wind speed was then calculated using Eq. (10). This procedure was repeated for wind speeds ranging from 50 mph (22 m/s) to 200 mph (89 m/s).

## 5. Results

The complementary fragilities (or survivorship curves) for roof sheathing failure can be plotted as complementary lognormal cumulative distributions:

$$\hat{S}(x) = 1 - Fr(x) = 1 - \Phi \left[ \frac{\ln(x) - \lambda_R}{\xi_R} \right] \quad (11)$$

<sup>2</sup> The panel failures are, in fact, *not* statistically independent events. The pressure field acting over the roof is spatially correlated and adjacent panel capacities may be correlated as a result of sharing a common roof framing member. In a series system, however, the assumption of independence is known to be conservative and permits the closed-form expressions given by Eqs. (8)–(10).

Table 5  
Lognormal parameters for roof sheathing fragilities

Baseline Structure	Exposure condition	Nail type and spacing	Damage level <sup>c,d,e,f</sup>	Wind direction					
				All directions		Normal-to-ridge direction		Parallel-to-ridge direction	
				$\lambda$	$\xi$	$\lambda$	$\xi$	$\lambda$	$\xi$
Structure Type 1	Exp B	6d nail <sup>a</sup> 6 in./12 in. (15.2 cm/ 30.5 cm)	level 1	4.353	0.0686	4.411	0.0670	4.372	0.0766
			level 2	4.383	0.0674	4.421	0.0586	4.401	0.0685
			level 3	4.410	0.0519	4.453	0.0439	4.459	0.0524
			level 4	4.492	0.0376	4.554	0.0376	4.608	0.0435
		8d nail <sup>b</sup> 6 in./12 in. (15.2 cm/30.5 cm)	level 1	4.680	0.0898	4.743	0.0935	4.718	0.0961
			level 2	4.734	0.0806	4.768	0.0726	4.762	0.0825
			level 3	4.770	0.0580	4.811	0.0517	4.826	0.0590
			level 4	4.862	0.0417	4.920	0.0414	4.983	0.0491
	Exp C	6d nail <sup>a</sup> 6 in./12 in. (15.2 cm/30.5 cm)	level 1	4.296	0.0675	4.356	0.0636	4.317	0.0754
			level 2	4.324	0.0633	4.366	0.0539	4.340	0.0626
			level 3	4.349	0.0493	4.393	0.0407	4.392	0.0477
			level 4	4.425	0.0348	4.484	0.0344	4.538	0.0396
		8d nail <sup>b</sup> 6 in./12 in. (15.2 cm/30.5 cm)	level 1	4.623	0.0911	4.683	0.0878	4.659	0.0934
			level 2	4.673	0.0783	4.709	0.0690	4.699	0.0778
			level 3	4.708	0.0551	4.750	0.0488	4.759	0.0558
			level 4	4.795	0.0396	4.855	0.0394	4.911	0.0458
	Exp D	6d nail <sup>a</sup> 6 in./12 in. (15.2 cm/30.5 cm)	level 1	4.205	0.0702	4.264	0.0647	4.221	0.0726
			level 2	4.229	0.0634	4.272	0.0550	4.245	0.0622
			level 3	4.256	0.0457	4.298	0.0405	4.298	0.0476
			level 4	4.331	0.0353	4.391	0.0345	4.444	0.0396
		8d nail <sup>b</sup> 6 in./12 in. (15.2 cm/30.5 cm)	level 1	4.530	0.0872	4.594	0.0888	4.563	0.0947
			level 2	4.578	0.0784	4.615	0.0705	4.605	0.0764
			level 3	4.613	0.0555	4.656	0.0491	4.665	0.0550
			level 4	4.701	0.0396	4.761	0.0393	4.817	0.0460
Structure Type 2	Exp B	6d nail <sup>a</sup> 6 in./12 in. (15.2 cm/30.5 cm)	level 1	4.236	0.0753	4.312	0.0727	4.257	0.0833
			level 2	4.296	0.0786	4.348	0.0667	4.319	0.0834
			level 3	4.339	0.0563	4.404	0.0465	4.425	0.0531
			level 4	4.446	0.0351	4.583	0.0436	4.627	0.0438
	Exp B	8d nail <sup>b</sup> 6 in./12 in. (15.2 cm/30.5 cm)	level 1	4.568	0.0938	4.648	0.0890	4.608	0.1010
			level 2	4.655	0.0939	4.704	0.0819	4.692	0.0964
			level 3	4.709	0.0596	4.773	0.0531	4.797	0.0595
			level 4	4.818	0.0384	4.958	0.0477	5.005	0.0487
	Exp C	6d nail <sup>a</sup> 6 in./12 in. (15.2 cm/30.5 cm)	level 1	4.181	0.0695	4.260	0.0652	4.199	0.0744
			level 2	4.230	0.0737	4.288	0.0625	4.253	0.0739
			level 3	4.276	0.0446	4.338	0.0419	4.355	0.0480
			level 4	4.377	0.0328	4.509	0.0400	4.554	0.0397
		8d nail <sup>b</sup> 6 in./12 in. (15.2 cm/30.5 cm)	level 1	4.506	0.0906	4.592	0.0892	4.546	0.0947
			level 2	4.590	0.0885	4.643	0.0776	4.623	0.0884
			level 3	4.643	0.0556	4.707	0.0490	4.726	0.0544
			level 4	4.749	0.0363	4.883	0.0443	4.931	0.0448

in which  $\Phi(\cdot)$  = standard normal cumulative distribution function,  $\lambda_R$  = logarithmic median of capacity  $R$  (in units that are dimensionally consistent with demand), and  $\xi_R$  = logarithmic standard deviation of capacity  $R$  (approximately equal to the coefficient of variation,  $V_R$ , when  $V_R < 0.3$ ). Fig. 3 shows that the complementary lognormal cumulative distribution provides a good fit to the calculated roof sheathing survivorship curves. The complementary fragility curves in Fig. 3 were developed for the Type 1 baseline structure using 8d common nails (0.131 in. (3.33 mm)

diameter, 2.5 in. (63.5 mm) long) spaced at 6 in. (150 mm) along the panel edge and 12 in. (300 mm) in the panel field, and located in Exposure C (open terrain). The survivorship (complementary fragility) can be viewed most simply as the limit state non-exceedence probability for a given wind speed (3 second gust wind speed at 33 ft. (10 m) above the ground in Exposure C). Table 5 summarizes the best-fit lognormal parameters for the roof sheathing complementary fragilities determined for the different baseline structures, exposure conditions, nail types, and system limit states.



Table 5 (continued)

Baseline Structure	Exposure condition	Nail type and spacing	Damage level <sup>c,d,e,f</sup>	Wind direction					
				All directions		Normal-to-ridge direction		Parallel-to-ridge direction	
				$\lambda$	$\xi$	$\lambda$	$\xi$	$\lambda$	$\xi$
Structure Type 3	Exp B	6d nail <sup>a</sup>	level 1	4.337	0.0661	4.350	0.0735	4.388	0.0797
		6 in./12 in.	level 2	4.418	0.0871	4.372	0.0644	4.443	0.0856
		(15.2 cm/30.5 cm)	level 3	4.443	0.0663	4.441	0.0438	4.506	0.0536
			level 4	4.511	0.0357	4.590	0.0391	4.648	0.0415
		8d nail <sup>b</sup>	level 1	4.665	0.0905	4.687	0.0953	4.732	0.0981
		6 in./12 in.	level 2	4.778	0.1012	4.730	0.0792	4.810	0.1011
		(15.2 cm/30.5 cm)	level 3	4.810	0.0728	4.807	0.0503	4.878	0.0633
			level 4	4.883	0.0395	4.968	0.0433	5.029	0.0461
	Exp C	6d nail <sup>a</sup>	level 1	4.279	0.0649	4.293	0.0698	4.332	0.0708
		6 in./12 in.	level 2	4.357	0.0807	4.313	0.0592	4.375	0.0737
		(15.2 cm/30.5 cm)	level 3	4.381	0.0629	4.377	0.0400	4.436	0.0446
			level 4	4.444	0.0355	4.518	0.0347	4.573	0.0366
		8d nail <sup>b</sup>	level 1	4.596	0.0898	4.630	0.0951	4.674	0.0968
		6 in./12 in.	level 2	4.702	0.0967	4.668	0.0748	4.742	0.0915
		(15.2 cm/30.5 cm)	level 3	4.731	0.0733	4.741	0.0474	4.807	0.0554
			level 4	4.805	0.0377	4.895	0.0398	4.954	0.0414
Structure Type 4	Exp B	6d nail <sup>a</sup>	level 1	4.746	0.0920	4.760	0.0860	4.795	0.0929
		6 in./12 in.	level 2	4.816	0.0872	4.861	0.1005	4.987	0.1461
		(15.2 cm/30.5 cm)	level 3	4.839	0.0660	4.880	0.0850	4.998	0.1371
			level 4	4.906	0.0420	4.948	0.0497	5.051	0.0997
	Exp C	8d nail <sup>b</sup>	level 1	4.690	0.0934	4.704	0.0853	4.738	0.0912
		6 in./12 in.	level 2	4.754	0.0833	4.796	0.0941	4.909	0.1288
		(15.2 cm/30.5 cm)	level 3	4.777	0.0661	4.816	0.0747	4.917	0.1208
			level 4	4.840	0.0399	4.875	0.0448	4.971	0.0790
Structure Type 5	Exp B	6d nail <sup>a</sup>	level 1	4.575	0.0940	4.591	0.0939	4.603	0.0937
		6 in./12 in.	level 2	4.665	0.0944	4.691	0.1039	4.695	0.1009
		(15.2 cm/30.5 cm)	level 3	4.710	0.0651	4.753	0.0652	4.764	0.0611
			level 4	4.802	0.0405	4.916	0.0518	4.915	0.0482
	Exp C	8d nail <sup>b</sup>	level 1	4.518	0.0844	4.531	0.0892	4.546	0.0943
		6 in./12 in.	level 2	4.601	0.0898	4.623	0.0952	4.627	0.0921
		(15.2 cm/30.5 cm)	level 3	4.647	0.0572	4.681	0.0600	4.693	0.0558
			level 4	4.734	0.0380	4.838	0.0479	4.839	0.0445

<sup>a</sup> 0.113 in. (2.87 mm) diameter, 2.0 in. (50.8 mm) long.

<sup>b</sup> 0.131 in. (3.33 mm) diameter, 2.5 in. (63.5 mm) long.

<sup>c</sup> Damage level 1 — no sheathing failures.

<sup>d</sup> Damage level 2 — no more than one sheathing panel failure.

<sup>e</sup> Damage level 3 — fewer than 10% of sheathing panels failed.

<sup>f</sup> Damage level 4 — fewer than 25% of sheathing panels failed.

Figs. 4–8 present selected roof system survivorship curves considering sheathing panel failure (removal). Fig. 4 presents a comparison of  $\hat{S}(x)$  curves for the different wind direction cases. (The “all directions” case includes the wind directionality factor.) Fig. 5 shows a comparison of  $\hat{S}(x)$  curves for the different system limit states, again considering all possible wind directions. The results in Figs. 4 and 5 are based on an analysis of baseline structure Type 1 (located in Exposure B) with sheathing attached using 6d common nails (0.113 in. (2.87 mm) diameter, 2.0 in. (50.8 mm) long). Roof sheathing survivorships vary with roof shape and slope, exposure condition, and nail size/schedule. Fig. 6 shows a comparison of  $\hat{S}(x)$  curves for

two different nail sizes (building Type 3 located in Exposure B). The effect of nail size on system failure probability is seen to be quite large. For example, considering building Type 3 located in Exposure B (Fig. 6), the probability of no panel failures when using 8d nails is about 75% when the basic wind speed is 100 mph. The corresponding failure probability when using 6d nails is negligible. These complementary fragilities illustrate the significant reduction in capacity when sheathing panels are attached using the smaller (6d) nail. Fig. 7 presents a comparison of  $\hat{S}(x)$  curves for different exposure conditions. Finally, Fig. 8 presents a comparison of  $\hat{S}(x)$  curves for the five different baseline structures. It may not be reasonable to compare

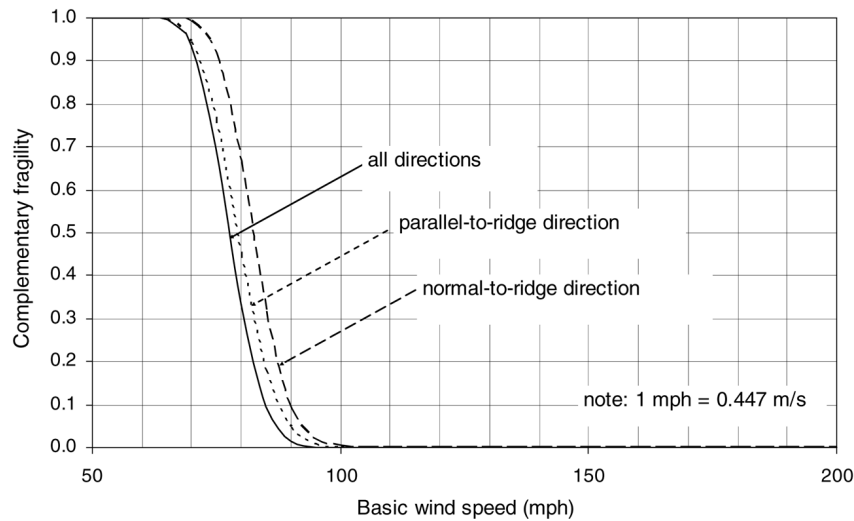


Fig. 4. Comparison of roof system survivorship curves for different wind directions (Structure Type 1/Exposure B/6d nail — 6 in./12 in. spacing) [damage level: no sheathing failure].

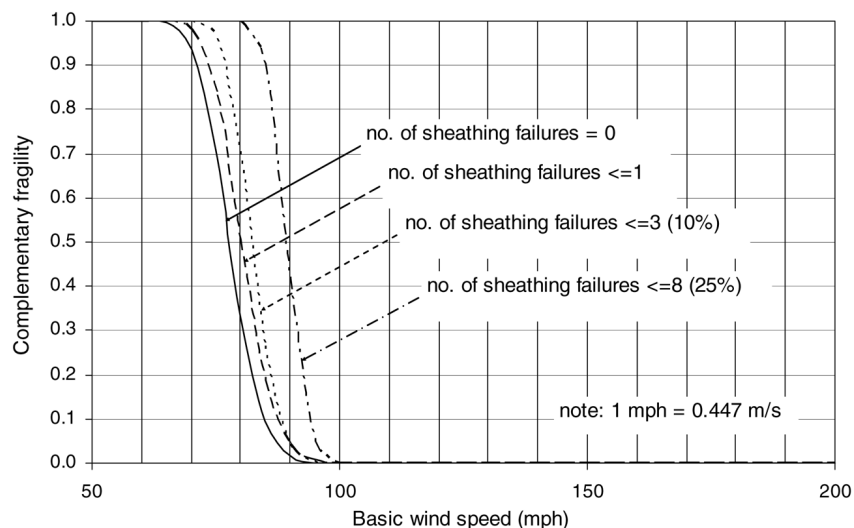


Fig. 5. Comparison of roof system survivorship curves for different damage levels (Structure Type 1/Exposure B/6d nail — 6 in./12 in. spacing) [all possible wind directions].

these curves directly since the structures have different roof configurations, panel layouts, etc. However, to the extent the structures are comparable, the effect of overhangs can be seen clearly. Complementary fragilities for the roofs with overhangs (Type 2, 3, and 5) are lower than those for roofs without overhangs. The roof system survivorship curves for the other baseline structures considering different exposure conditions, nail types, wind direction profiles, and system limit states may be found elsewhere [8]. In most cases, the  $\hat{S}(x)$  curves considering all possible wind directions are lower than those for the directional cases (normal-to-ridge and parallel-to-ridge). This might suggest that current directionality factors for components and cladding are conservative.

## 6. Conclusions

This paper presented selected results of a study to develop roof sheathing fragility and complementary fragility (survivorship) curves for low rise woodframe structures built in high wind regions. Five simple baseline woodframe structures, representative of residential construction in the southeast United States, were considered. Roof sheathing survivorship curves were developed for each baseline structure considering four different damage limit states (per cent sheathing removal) as well as different wind directionality profiles, nail types, and exposure conditions. The complementary fragilities were found to be well fit by a complementary lognormal cumulative distribution. Selected

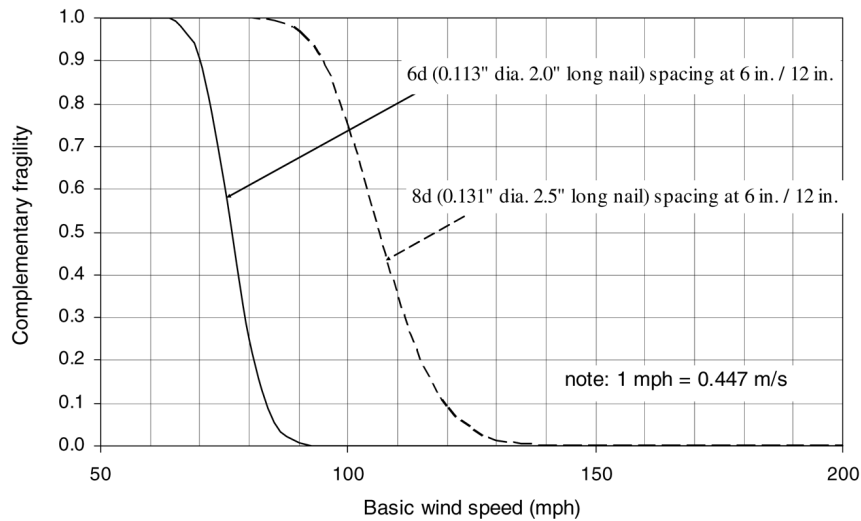


Fig. 6. Comparison of roof system survivorship curves for different nail types (Structure Type 3/Exposure B/all possible wind directions) [damage level: no sheathing failures].

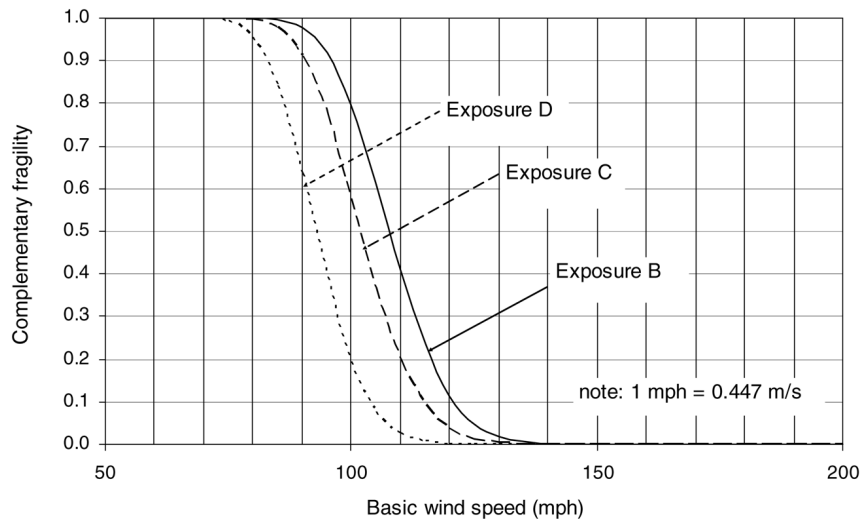


Fig. 7. Comparison of roof system survivorship curves for different exposures (Structure Type 1/8d nail — 6 in./12 in. spacing/all possible wind directions) [damage level: no sheathing failures].

results were presented in this paper, while more complete results may be found elsewhere [8].

The fragility methodology described herein can be used to develop performance-based design guidelines for woodframe structures in high wind regions as well as to provide information on which to base structural safety or expected loss (structural, economic) assessments. Fragilities (or complements of survivorships) such as those presented here also can be convolved with appropriate wind speed hazard (demand) functions to evaluate failure probabilities for the different damage levels. The fragility methodology in this study can be used to predict roof sheathing performance, improve the reliability of roof systems designed to resist high wind loads and (when coupled with a loss model) predict economic loss due to roof sheathing failure and

quantify the role of building envelope integrity. In order for fragility curves such as those developed in this study to reach their fullest potential as design and/or assessment tools, they will need to be properly validated using post-disaster damage survey data.

### Acknowledgements

This work was conducted while the authors were Graduate Research Assistant and Professor, respectively, at Oregon State University. The research described in this paper was supported by funds from the National Science Foundation (Grant No. CMS-0049038) and the Richardson Chair Endowment in the Department of Wood Science and Engineering at Oregon State University. This

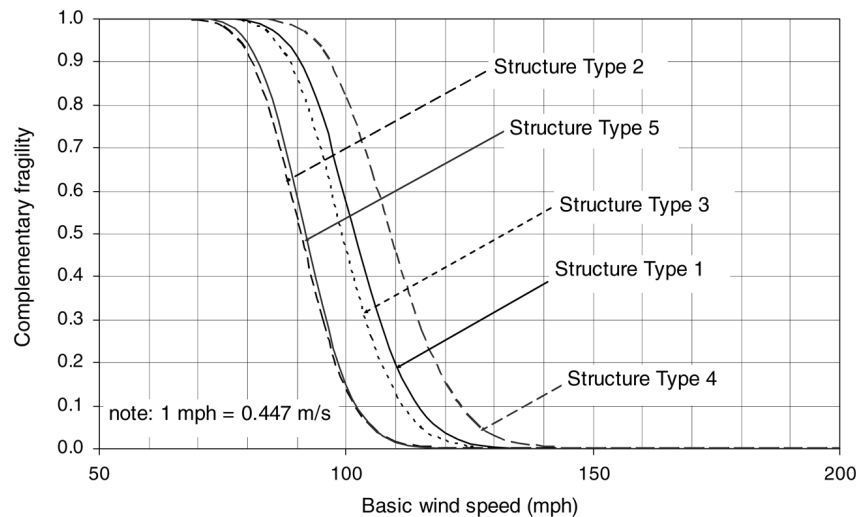


Fig. 8. Comparison of roof system survivorship curves for different baseline structures (Exposure C/8d nail — 6 in./12 in. spacing/all possible wind directions) [damage level: no sheathing failures].

support is gratefully acknowledged. The authors take sole responsibility for the views expressed in this paper, which may not represent the position of the National Science Foundation, Oregon State University, or Texas A&M University.

## References

- [1] ASCE. Minimum design loads for buildings and other structures, Standard ASCE 7-02. Reston, VA: Structural Engineering Institute of the American Society of Civil Engineers; 2002.
- [2] Cook NJ. The designer's guide to wind loading of building structures – Part 2 static structures. Borough Green, Sevenoaks, Kent TN15 8PH, England: Butterworths; 1985.
- [3] Ellingwood BR, Galambos TV, MacGregor JG, Cornell CA. Development of a probability based load criterion for American national standard A58. Washington (DC): U.S. Department of Commerce, National Bureau of Standards; 1980 [Special Publication 577].
- [4] Ellingwood BR, Tekie PB. Wind load statistics for probability-based structural design. *Journal of Structural Engineering*, ASCE 1999; 125(4):453–63.
- [5] Ellingwood BR, Rosowsky DV, Li Y, Kim JH. Fragility assessment of light-frame construction subjected to wind and earthquake hazards. *ASCE* 2004;130(12):1921–30.
- [6] Holmes JD. Wind pressures on tropical housing. *Journal of Wind Engineering and Industrial Aerodynamics* 1994;53:105–23.
- [7] Kennedy RP, Ravindra MK. Seismic fragilities for nuclear power plant studies. *Nuclear Engineering and Design* 1984;79(1):47–68.
- [8] Lee KH. 2004, Site-specific hazards and load models for probability-based design. Ph.D. dissertation, Department of Civil, Construction, and Environmental Engineering, Oregon State University, Corvallis, OR.
- [9] NAHB. Housing affordability through design efficiency program. Upper Marlboro (MD): NAHB Research Center Inc.; 1997.
- [10] Rosowsky DV, Cheng N. Reliability of light-frame roofs in high-wind regions. I: wind loads. *Journal of Structural Engineering*, ASCE 1999; 125(7):725–33.
- [11] Rosowsky DV, Cheng N. Reliability of light-frame roofs in high-wind regions. II: Reliability analysis. *Journal of Structural Engineering*, ASCE 1999;125(7):734–9.
- [12] Rosowsky DV, Ellingwood BR. Performance-based engineering of wood frame housing: Fragility analysis methodology. *Journal of Structural Engineering*, ASCE 2002;128(1):32–8.
- [13] Rosowsky DV, Kim JH. Reliability studies. Richmond (CA): Consortium of Universities for Research in Earthquake Engineering; 2002 [CUREE Publication No. W-10].
- [14] Rosowsky DV, Schiff SD. Probabilistic modeling of roof sheathing uplift capacity. In: *Proceedings: ASCE specialty conference on probabilistic mechanics and structural reliability*. 1996, p. 334–7.
- [15] Xu YL, Reardon GF. Variations wind pressure on hip roofs with roof pitch. *Journal of Wind Engineering and Industrial Aerodynamics* 1998;73:267–84.